

# Sectm1a deficiency aggravates inflammation-triggered cardiac dysfunction through disruption of LXR $\alpha$ signalling in macrophages

Yutian Li<sup>1</sup>, Shan Deng <sup>2</sup>, Xiaohong Wang<sup>1</sup>, Wei Huang<sup>3</sup>, Jing Chen<sup>4,5</sup>, Nathan Robbins<sup>6</sup>, Xingjiang Mu<sup>1</sup>, Kobina Essandoh<sup>1</sup>, Tianqing Peng<sup>7</sup>, Anil G. Jegga <sup>4</sup>, Jack Rubinstein<sup>6</sup>, David E. Adams<sup>8</sup>, Yigang Wang<sup>3</sup>, Jiangtong Peng<sup>2\*</sup>, and Guo-Chang Fan <sup>1\*</sup>

<sup>1</sup>Department of Pharmacology and Systems Physiology, University of Cincinnati College of Medicine, 231 Albert Sabin Way, Cincinnati, OH 45267-0575, USA; <sup>2</sup>Department of Cardiology, Union Hospital, Tongji Medical College, Huazhong University of Science and Technology, Wuhan, Hubei 430022, China; <sup>3</sup>Department of Pathology and Laboratory Medicine, University of Cincinnati College of Medicine, 231 Albert Sabin Way, Cincinnati, OH 45267-0575, USA; <sup>4</sup>Division of Biomedical Informatics, Cincinnati Children's Hospital, Cincinnati, OH 45267, USA; <sup>5</sup>Department of Pediatrics, University of Cincinnati College of Medicine, 231 Albert Sabin Way, Cincinnati, OH 45267-0575, USA; <sup>6</sup>Department of Internal Medicine, University of Cincinnati College of Medicine, 231 Albert Sabin Way, Cincinnati, OH 45267-0575, USA; <sup>7</sup>Critical Illness Research, Lawson Health Research Institute, London, ON N6A 4G5, Canada; and <sup>8</sup>Division of Immunology, Allergy and Rheumatology, University of Cincinnati College of Medicine, 231 Albert Sabin Way, Cincinnati, OH 45267-0575, USA

Received 20 November 2019; revised 17 February 2020; editorial decision 7 March 2020; accepted 12 March 2020; online publish-ahead-of-print 14 March 2020

Time for primary review: 37 days

## Aims

Cardiac dysfunction is a prevalent comorbidity of disrupted inflammatory homeostasis observed in conditions such as sepsis (acute) or obesity (chronic). Secreted and transmembrane protein 1a (Sectm1a) has previously been implicated to regulate inflammatory responses, yet its role in inflammation-associated cardiac dysfunction is virtually unknown.

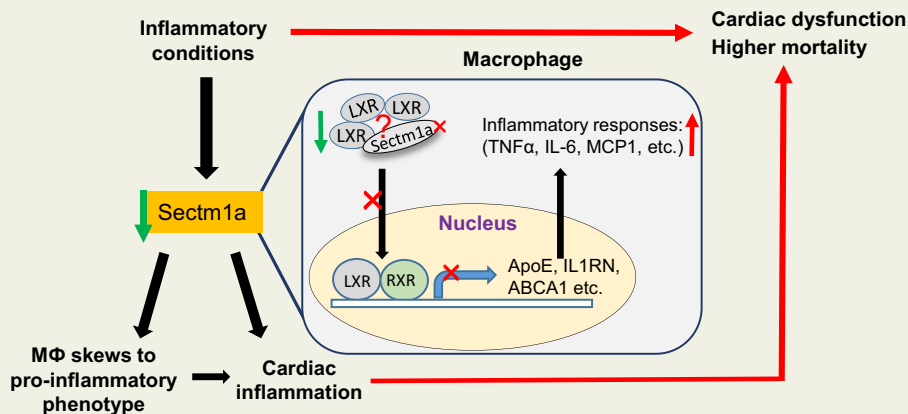
## Methods and results

Using the CRISPR/Cas9 system, we generated a global Sectm1a-knockout (KO) mouse model and observed significantly increased mortality and cardiac injury after lipopolysaccharide (LPS) injection, when compared with wild-type (WT) control. Further analysis revealed significantly increased accumulation of inflammatory macrophages in hearts of LPS-treated KO mice. Accordingly, ablation of Sectm1a remarkably increased inflammatory cytokines levels both *in vitro* [from bone marrow-derived macrophages (BMDMs)] and *in vivo* (in serum and myocardium) after LPS challenge. RNA-sequencing results and bioinformatics analyses showed that the most significantly down-regulated genes in KO-BMDMs were modulated by LXR $\alpha$ , a nuclear receptor with robust anti-inflammatory activity in macrophages. Indeed, we identified that the nuclear translocation of LXR $\alpha$  was disrupted in KO-BMDMs when treated with GW3965 (LXR agonist), resulting in higher levels of inflammatory cytokines, compared to GW3965-treated WT-cells. Furthermore, using chronic inflammation model of high-fat diet (HFD) feeding, we observed that infiltration of inflammatory monocytes/macrophages into KO-hearts were greatly increased and accordingly, worsened cardiac function, compared to WT-HFD controls.

## Conclusion

This study defines Sectm1a as a new regulator of inflammatory-induced cardiac dysfunction through modulation of LXR $\alpha$  signalling in macrophages. Our data suggest that augmenting Sectm1a activity may be a potential therapeutic approach to resolve inflammation and associated cardiac dysfunction.

## Graphical Abstract



## Keywords

Macrophage • Inflammation • Cardiac function • Cardiac inflammation • LXR

## 1. Introduction

Acute and chronic dysregulation of inflammatory homeostasis contribute to comorbidities associated with a wide variety of diseases.<sup>1,2</sup> For instance, in experimental animal model or human endotoxaemia model, acute activation of immune cells by inflammatory factors [i.e. lipopolysaccharide (LPS, a natural adjuvant synthesized by Gram-negative bacteria)] elicits profound effects on immune responses,<sup>3,4</sup> whereas extensive studies have shown that obesity is associated with a chronic, low-grade inflammatory state.<sup>5,6</sup> In both scenarios, there are systemically greater abundance of pro-inflammatory cytokines and increased infiltration and activation of immune cells in various tissues.

Cardiac dysfunction is a common feature associated with both acute and chronic inflammatory states. Indeed, septic patients with cardiac dysfunction show about 40% higher mortality rate when compared with patients without contractile abnormalities<sup>7,8</sup>; while obesity has long been recognized as an independent risk factor for many chronic diseases including cardiovascular disease and diabetes.<sup>9–11</sup> As a fundamental component of innate immunity, macrophages play critical roles in both initiating and resolving inflammation in the heart. In fact, macrophages are prominent cells that drive septic cardiomyopathy in preclinical animal models<sup>12,13</sup>; and human monocytes and macrophages correlate with atherosclerosis severity and secrete more inflammatory cytokines in type 2 diabetic patients.<sup>14,15</sup> Nevertheless, how macrophages contribute to cardiac inflammation and subsequent injury is still incompletely understood.

Nuclear receptors are intracellular transcription factors that are expressed in a wide variety of cells. They can interact with DNA directly to regulate many biological processes including cardiovascular function, immune response, and lipid metabolism of organism.<sup>16,17</sup> The Liver X Receptors (LXR $\alpha$  and LXR $\beta$ ) belong to the adopted orphan nuclear receptor family, and they have been identified as critical regulators linking inflammation and lipid metabolism.<sup>18</sup> While LXR $\beta$  is ubiquitously expressed, LXR $\alpha$  is dominantly expressed in liver and macrophages.<sup>19,20</sup> Apart from regulating cholesterol and fatty acid

homeostasis, extensive studies have shown that LXRs have robust anti-inflammatory activity, which is mediated by various mechanisms such as inhibition of NF- $\kappa$ B pathway or modification of plasma membrane composition to disrupt inflammatory signal transduction.<sup>18,20–22</sup> Furthermore, activation of toll-like receptors could inhibit LXR function,<sup>23</sup> and animal model with LXR deficiency are more susceptible to LPS- or bacterial-induced illness, which can be rescued by LXR agonist, such as GW3965.<sup>24,25</sup>

Human secreted and transmembrane 1 (Sectm1), also known as K12, is a transmembrane and secreted protein with characteristics of a type 1a transmembrane protein of SECTM family.<sup>26</sup> Sectm1 is highly expressed in cells of the myeloid lineage and epithelia where its expression is up-regulated by STAT1-dependent and NF- $\kappa$ B RelA-independent mechanisms.<sup>27</sup> The mouse genome contains two Sectm1 genes, Sectm1a and 1b, with the greatest homology between mouse Sectm1a and human Sectm1.<sup>28</sup> Both human Sectm1 and mouse Sectm1a have been implicated as an alternative CD7 ligand to stimulate T-cell proliferation and attract human monocytes.<sup>28,29</sup> However, Sectm1a has also been speculated to stimulate diverse receptors, including glucocorticoid-induced TNF receptor (GITR), aforementioned CD7, and additional ones yet to be identified, but its function remains largely unexplored.<sup>27,28</sup> Recently, Kamata *et al.*<sup>27</sup> observed that Sectm1a was one of the most highly expressed proteins in epithelial cells from pneumonia-infected lungs; it was found to be preferentially bound to neutrophils in infected lung and up-regulated chemokine CXCL2 expression; and Huyton *et al.* reported that expression of Sectm1 in human monocytes was negatively regulated by LPS.<sup>30</sup> Given the pronounced effects of monocyte/macrophages in cardiac inflammatory homeostasis, we aimed to investigate the functional role of Sectm1a in macrophages. By combining *in vivo* and *in vitro* loss- [global knockout (KO) mouse model] and gain-of-function (overexpression through adenovirus infection) studies, we demonstrate that Sectm1a is a critical repressor of inflammation by activating LXR $\alpha$  pathway. Our results support the hypothesis that deficiency of Sectm1a promotes inflammatory macrophage phenotype and subsequently impairs cardiac contractile function.

## 2. Methods

### 2.1 Animals and treatments

The global Sectm1a-KO mouse model was generated using the CRISPR/Cas9 system in C57BL/6 background mice by the Division of Developmental Biology at Cincinnati Children's Hospital Medical Center (Supplementary material online, Figure S1A). Mice were maintained and bred in the Division of Laboratory Animal Resources at the University of Cincinnati Medical Center. All animal experiments conformed to the Guidelines for the Care and Use of Laboratory Animals prepared by the National Academy of Sciences, published by the National Institutes of Health, and approved by the University of Cincinnati Animal Care and Use Committee (Protocol #07-07-06-01). C57BL/6 wild-type (WT) mice were used as control; 10- to 12-week-old sex-matched mice were studied if not specified elsewhere. For acute inflammatory model, animals received 10 mg/kg body weight (BW) of LPS (from *Escherichia coli* O111:B4, #L2630, Sigma-Aldrich) intraperitoneally (*i.p.*) in 0.2 mL saline. The survival rate of WT and KO mice were monitored every 6 h for a 72 h period after LPS injection. For LXR agonist experiment, mice received three doses of GW3965 (30 mg/kg of BW, once daily, DMSO used as control, *i.p.*), 6 h after the last GW3965 injection, all mice were injected with LPS, followed by echocardiography measurement 12 h post-LPS injection. For chronic inflammatory model, mice were fed with high-fat diet (HFD) (ResearchDiet, Cat. # D12492; 60% kcal from fat, 20% kcal from protein, and 20% kcal from carbohydrate) starting at age of 5–6 weeks for 18–24 weeks. Mice were anaesthetized by one intraperitoneal (*i.p.*) injection of ketamine (90 mg/kg BW) and xylazine (20 mg/kg of BW), depth of anaesthesia was monitored by toe pinch.

### 2.2 Culture and treatment of bone marrow-derived macrophages from WT and Sectm1a-KO mice or RAW264.7 macrophages

L929 cell line was purchased from ATCC and cultured in normal complete DMEM (15% FBS, 1% penicillin/streptomycin solution), cell culture medium was collected after 10 days of culture and centrifuged at 750 g for 10 min, supernatant was then stored at -20°C until use. Bone marrow-derived macrophages (BMDMs) were isolated and cultured as described previously.<sup>31,32</sup> In brief, WT and Sectm1a-KO mice were euthanized using carbon dioxide followed by removal of both hind legs. Skin and muscle were removed and bones were washed twice in ice cold PBS. By using 25G needle filled with cold sterile wash medium (DMEM without calcium and magnesium), bone marrow was flushed out and filtered through 70 µm Nylon cell strainer. Then cells were centrifuged at 500 g for 5 min at room temperature (RT), followed by resuspension of cell pellet in Red Blood Cell (RBC) lysis buffer for 5 min, and then centrifuged again. The resulting cell pellet was re-suspended in complete culture medium (DMEM supplemented with 15% L929 cell culture supernatant, 10% FBS, 1% penicillin/streptomycin solution). Cells were allowed to grow and differentiate for 7 days.

Mouse macrophage cell line RAW264.7 were purchased from American Type Culture Collection (ATCC), Rockville, MD, USA and cultured in normal complete DMEM. All cells were grown at 37°C with 5% CO<sub>2</sub> in fully humidified air. Before any treatment, cells (RAW264.7 macrophages or BMDMs) were plated in 6-well plates (3 × 10<sup>5</sup> cells/well seeding density) or 24-well plates (5 × 10<sup>4</sup> cells/well seeding density) and allowed to adhere for 24 h. After two washes with PBS, cells were treated with LPS (from *E. coli* O111:B4, #L4391, Sigma-Aldrich) or

palmitate (#P0500, Sigma-Aldrich) at indicated doses and time points specified in Section 3 and Fig.1, Fig. 3, Fig. 6A-G, and Fig. 7A-C. PBS or endotoxin-free bovine serum albumin (BSA) were used as control, respectively. Culture supernatant was then collected for cytokine measurement and cells were collected for qPCR. For Sectm1a overexpression experiments, BMDMs were infected with recombinant adenoviruses (Ad.Sectm1a or Ad.GFP) at 500 MOI for 48 h, followed by LPS (10 ng/mL) treatment for 8 h. Cell culture supernatant was collected for cytokine measurement by ELISA.

### 2.3 Isolation and treatment of adult rat cardiomyocytes

After anaesthetized by one *i.p.* injection of ketamine (80 mg/kg BW) and Xylazine (10 mg/kg BW), adult rat ventricular myocytes were isolated from Langendorff-perfused hearts of 6-week-old male Sprague-Dawley rats (The Jackson Laboratory, Bar Harbor, ME) as described before.<sup>33</sup> Cardiomyocytes were plated on laminin (10 µg/mL) coated 6-well plates overnight, followed by infection with adenoviruses (Ad.Sectm1a or Ad.GFP) at 100 MOI. After 24 h, cardiomyocytes were then treated with LPS (50 ng/mL) for 3 h, and cells were then harvest for qRT-PCR analysis.

### 2.4 RNA isolation and quantitative RT-PCR

Quantitative real-time PCR (qRT-PCR) was performed as described previously.<sup>34</sup> Total RNA was extracted from cultured cells or tissues using the RNeasy kit (Qiagen, Cat. 217004) in accordance with the manufacturer's instructions. cDNA was synthesized from 1.0 µg RNA using Superscript II Reverse Transcriptase (Invitrogen, Cat. 18080044). Then qRT-PCR was performed in triplicate with the ABI PRISM 7900HT sequence detection system (ABI) using SYBR green (Genecopoeia, Cat. QP005). Relative mRNA levels were calculated using the delta CT method and normalized to GAPDH as internal control. Sequences of primers used for quantitative RT-PCR are listed in Supplementary material online, Table S4. Directional polyA RNA-sequencing was performed by the Genomics, Epigenomics and Sequencing Core (GESCC) at the University of Cincinnati.

### 2.5 Cytokine measurement in peripheral blood and cell culture supernatants

Whole blood samples were collected by cardiac puncture with heparinized needles at indicated time points after LPS injection, and spun down at 4000 rpm for 10 min. Cell culture supernatants from macrophages were harvested at different time points with different treatment schemes. The levels of tumour necrosis factor (TNF)-α, interleukin (IL)-6, IL-1β, and MCP-1 in the sera and culture supernatants were measured, using commercially available ELISA kits [BioLegend, Cat. 430901 (TNFα), 431301 (IL-6), 432601 (IL-1β), 432702 (MCP-1)], according to manufacturer's protocol.

### 2.6 Flow cytometry analysis

Methods for analysing macrophages with flow cytometry were adopted from previous studies with modifications.<sup>32,35,36</sup> In brief, heart tissue was minced and digested in HBSS with Collagenase IV (2 mg/mL, Worthington, #LS004188), Dispase II (1.2 U/mL, Sigma, #D4693), and 0.9 mM CaCl<sub>2</sub>, then incubated at 37°C for 45 min. with gentle agitation. Tissues were then passed through 40 µm cell strainer followed by centrifugation at 500 g at 4°C for 5 min. The pellets were resuspended in flow cytometry sorting buffer (HBSS with 1 mM EDTA, 25 mM HEPES and

1% FBS) and incubated on ice with Fc-blocking solution (anti-CD16/32, eBioScience, Cat. #14-0161-81, 1:100 dilution) for 10 min. After washing, cells were stained with primary antibodies (listed in [Supplementary material online, Table S5](#)) at 4°C for 30 min in dark. Then cells were washed twice, fixed in 0.1% PFA for 15 min., and flow cytometry was performed using LSRII Analyzer (SHC Flow Cytometry Core, Cincinnati), and analysed with FCSEXpress software.

## 2.7 Histology analysis

Heart samples were harvested and immediately fixed in 10% neutral buffered formalin (Sigma-aldrich, HT501128) at 4°C for at least 48 h, and then embedded in paraffin. Heart sections were made and deparaffinized in xylene, followed by rehydration through graded ethanol (100%, 95%, 75%, 50%). After rinsing with distilled water, sections were subjected to heat-mediated antigen retrieval with sodium citrate buffer (0.01 M, pH 6.0, 95°C, 15 min). For cell staining, BMDMs were washed with PBS 3 times and fixed with 4% PFA for 15 min at RT, followed by another three wash of PBS. Then samples (cells or tissue section) were blocked with 1% BSA solution at RT for 1 h. Next, sections were incubated with primary antibodies: F4/80 (Biolegend, #123101),  $\alpha$ -actinin (Sigma, #A7811), or LXR $\alpha$  (Invitrogen, #PA1-330) overnight at 4°C. After washing with PBS, samples were incubated with secondary antibodies at RT for 1 h, and then mounted with Antifade Mountant medium (Invitrogen, Cat.# P36962). Images were captured with Zeiss LSM710 LIVE Duo Confocal Microscope (Live Microscopy Core, University of Cincinnati).

## 2.8 Assessment of cardiac function in vivo

Cardiac function was assessed *in vivo* using trans-thoracic echocardiography (Vevo<sup>®</sup> 2100 Imaging System, Visualsonics) with a M5400 probe (30-MHz centerline frequency) in 1.5% isoflurane anaesthetized mice. Left ventricular end-diastolic (LVIDD) and end-systolic diameters (LVIDs) were measured from M-mode recordings. Left ventricular ejection

fraction (EF) was calculated as:  $[(LVDD^3 - LVDs^3)/LVDD^3] \times 100$ . All measurements were performed according to the American Society for Echocardiography leading-edge technique standards, and averaged over at least three consecutive cardiac cycles.

## 2.9 Statistical analysis

Data were expressed as means  $\pm$  SEM. Comparison between two groups was determined by Student's *t*-test. Differences among multiple groups were determined by one- or two-way ANOVA where appropriate. The survival rates were constructed using the Kaplan–Meier method, and differences in mortality were compared using the log-rank test. A *P* < 0.05 was considered statistically significant.

## 3. Results

### 3.1 Kinetics of LPS-stimulated gene expression of Sectm1a

Sectm1a is highly expressed in multiple tissues such as spleen or stomach ([Supplementary material online, Figure S1B](#)) and cells of the myeloid lineage and epithelia.<sup>27,28</sup> Yet, whether Sectm1a plays any role in macrophages remains unknown. To this end, we first determined whether the expression of Sectm1a in macrophages was altered in response to endotoxin (i.e. LPS) challenge. After culturing BMDMs with different doses of LPS for 24 h, Sectm1a gene expression was profoundly reduced when comparing to PBS control group ([Figure 1A](#)); whereas Sectm1b levels showed no significant difference ([Supplementary material online, Figure S1C](#)). In addition, we observed that LPS was able to up-regulate Sectm1a expression in WT BMDMs at early time points (peak at 6 h), whereas being significantly reduced after 24 h ([Figure 1B](#)). Given that Sectm1a is highly abundant in the spleen and the blood, we next measured its mRNA levels in whole blood and spleen from WT mice after LPS injection. Intriguingly, Sectm1a levels were dramatically reduced in whole

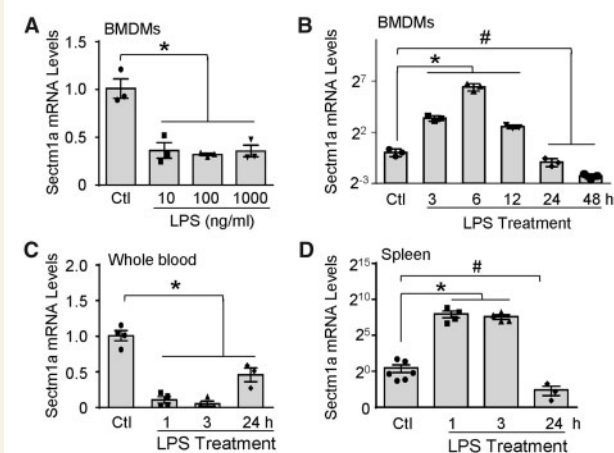


**Figure 1** Kinetics of LPS-stimulated gene expression of Sectm1a. (A and B) Gene expression of Sectm1a was measured in WT BMDMs treated with indicated doses of LPS (A) for 24 h or with LPS (10 ng/mL) for indicated time points (B) (*n* = 3). (C and D) WT mice were *i.p.* injected with LPS (10 mg/kg of BW), Sectm1a mRNA levels in whole blood (C) and spleen (D) were determined at various time points (*n* = 3–5) (\* and # *P* < 0.05; data are presented as mean  $\pm$  SEM; Student's *t*-test).

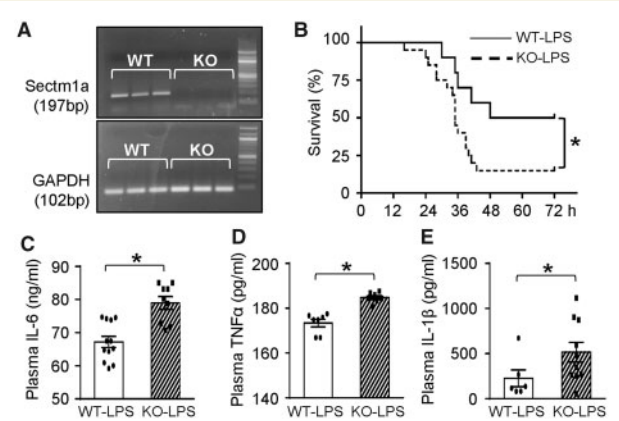


**Figure 2** Sectm1a deficiency aggravates LPS-induced systemic inflammation and mortality. (A) Products of qRT-PCR were run on agarose gel to validate that Sectm1a KO model was successfully generated. (B) WT and Sectm1a KO mice injected *i.p.* with LPS (10 mg/kg) were monitored for survival up to 72 h post-treatment. *n* = 10–20. (C–E) Plasma cytokine levels (C: IL-6; D: TNF $\alpha$ ; E: IL-1 $\beta$ ) of WT and Sectm1a KO mice were measured with ELISA 12 h after LPS injection (number of serum samples: *n* = 9–12 for C; *n* = 7 for D; *n* = 6–10 for E) (\**P* < 0.05; data are presented as mean  $\pm$  SEM; Student's *t*-test).

blood but increased in spleen at 1 h and 3 h post-LPS injection; after 24 h, mRNA levels of Sectm1a were greatly lower in both tissues when compared with PBS control group (Figure 1C and D). Put together, these data suggest that Sectm1a may be involved in the activation of LPS-stimulated inflammatory responses, and its up-regulation at the early phase of inflammation could act as a compensatory mechanism.

### 3.2 Sectm1a deficiency aggravates LPS-induced systemic inflammation and mortality

Since Sectm1 is ubiquitously expressed and could be secreted in truncated form,<sup>26</sup> we generated a global (instead of a cell/tissue-specific) KO mouse model using CRISPR-Cas9 technology. We validated that the expression of Sectm1a was deficient but Sectm1b expression was not affected (Figure 2A and Supplementary material online, Figure S2). These mice bred normally and are behaviourally similar to WT controls. To explore the potential role(s) of Sectm1a in inflammatory conditions, both WT and KO mice received LPS injection (10 mg/kg of BW, *i.p.*). We observed about 40% higher mortality rate in KO mice with median survival of 35 h (median survival for WT mice: 60 h,  $n = 10-20$ ) during 72 h of LPS treatment (Figure 2B). Next, we measured the levels of pro-inflammatory cytokines in sera at 12 h post-LPS injection. As shown in Figure 2C–E, loss of Sectm1a significantly increased serum levels of IL-6, TNF $\alpha$ , and IL-1 $\beta$ , when compared with WT-LPS group. Put together, these data indicate that Sectm1a may be a pivotal mediator in the regulation of LPS-induced inflammatory responses.

### 3.3 Ablation of Sectm1a leads to exacerbated cardiac inflammation and dysfunction

It is well-recognized that systemic inflammatory response initiated by bacterial endotoxin can directly impair cardiac function,<sup>12</sup> thus, we assessed cardiac function at 12 h post-LPS injection using echocardiography. The results showed that Sectm1a-KO mice exhibited normal cardiac function similar to WT controls under basal conditions (PBS injection) (Figure 3A and B and Supplementary material online, Table S1). However, in comparison to WT-LPS group, Sectm1a-KO mice showed further aggravated cardiac dysfunction after LPS injection, as evidenced by 38% reduction in fractional shortening (Figure 3B and Supplementary material online, Table S1). Given that cardiac dysfunction may be at least partially attributed to increased infiltration of immune cells into the myocardium,<sup>37</sup> we next went on to determine the types and numbers of immune cells in LPS-treated mouse hearts, using flow cytometry analysis and immunofluorescent staining. As shown in Figure 3C/G, D/H and Supplementary material online, Figure S3A–C, the number of macrophages and neutrophils were dramatically increased in LPS-treated KO hearts, when compared with LPS-treated WT group. More interestingly, these macrophages from KO-LPS hearts displayed proinflammatory phenotype with higher expression of CCR2 and MHC-II but reduced levels of CD206 (Figure 3E/I and F/J), compared to those cells from WT-LPS hearts. Accordingly, levels of TNF $\alpha$ , IL-6, and IL-1 $\beta$  were significantly higher in heart homogenates of KO mice than those of WT-LPS mice at 12 h post-LPS injection (Figure 3K–M). Altogether, these data suggest that Sectm1a may be a critical factor to resist inflammatory insult in the heart and thereby preserve cardiac function.

### 3.4 Lack of Sectm1a augments LPS-induced inflammation via skewing BMDMs towards pro-inflammatory phenotype

To define the functional role of Sectm1a in LPS-stimulated macrophages in a cell-autonomous manner, BMDMs were isolated from WT and Sectm1a-KO mice. As shown in Figure 4A, no difference was observed on differentiation, proliferation, and morphology of BMDMs from WT and KO mice. Also, Sectm1a deficiency did not alter the basal levels of inflammatory factors, such as TNF $\alpha$ , IL-1 $\beta$ , IL-6, and MCP-1 (Figure 4B–E). However, in LPS-treated BMDMs, lack of Sectm1a significantly augmented the secretion of these inflammatory factors at 24 h (Figure 4B–E), though only marginal increase in IL-6 levels was observed in KO-BMDMs at 12 h time point, when compared with WT-BMDMs (Figure 4D). In consistence with the cytokine profile, flow cytometry analysis revealed 31% higher but 24% lower in the levels of CD38 (proinflammatory marker) and CD206 (anti-inflammatory marker), respectively, in KO-BMDMs at 6 h post-LPS treatment (Figure 4F). These data indicate that deletion of Sectm1a skews macrophages towards pro-inflammatory phenotype. Since activation of NF- $\kappa$ B pathway is the major mechanism to regulate inflammatory responses in LPS-treated macrophages, and phosphorylation of the key subunit, p65, could stimulate the downstream transcriptional signals,<sup>38,39</sup> we sought to examine whether Sectm1a deficiency could promote LPS-induced NF- $\kappa$ B activation in macrophages. As shown in Figure 4G, phosphorylation of p65 was further increased by 48% in Sectm1a-KO BMDMs 30 min after LPS exposure, when compared with WT-LPS controls. Moreover, we observed a marked increase in I $\kappa$ B $\alpha$  phosphorylation at S32/36, a key regulator of p65 activity, in KO-BMDMs after LPS treatment, when compared with WT-LPS group (Figure 4G). On the other hand, we showed that overexpression of Sectm1a in BMDMs via adenovirus could significantly reduce LPS-triggered phosphorylation of p65 and I $\kappa$ B $\alpha$  (Supplementary material online, Figure S4A–C), when compared with Ad.GFP control group with LPS treatment. Subsequently, production of inflammatory cytokines was markedly reduced in BMDMs with Sectm1a overexpression (Supplementary material online, Figure S4D–G). Importantly, when Sectm1a was up-regulated in adult rat cardiomyocytes using the same adenovirus, mRNA levels of cytokines (IL-6 and IL-1 $\beta$ ) showed no differences (Supplementary material online, Figure S4H and I), indicating that Sectm1a does not regulate inflammatory response in cardiomyocytes. Overall, these data suggest that Sectm1a deficiency enhances inflammation in macrophages through the activation of NF- $\kappa$ B pathway.

### 3.5 Gene enrichment analysis of Sectm1a-KO BMDMs

To further identify potential mechanisms underlying the aberrant inflammatory responses in Sectm1a-KO macrophages, we performed RNA-sequencing analyses of the gene expression profile in BMDMs isolated from WT and Sectm1a-KO mice (Figure 5A). Among the 714 up-regulated and 746 down-regulated genes in Sectm1a-KO BMDMs (Figure 5B), 75 differentially expressed genes are involved in cytokine-cytokine receptor interaction and chemokine signalling pathways (Supplementary material online, Figure S5A). Interestingly, many of the most significantly down-regulated genes are directly or indirectly regulated by LXR signalling pathway, such as ApoE, Plin2, IL-1RN, Cebp $\alpha$ , and ABCA1 (Figure 5C–E). More intriguingly, gene expression of LXR $\alpha$  itself was significantly reduced in KO-BMDMs, when compared with WT-

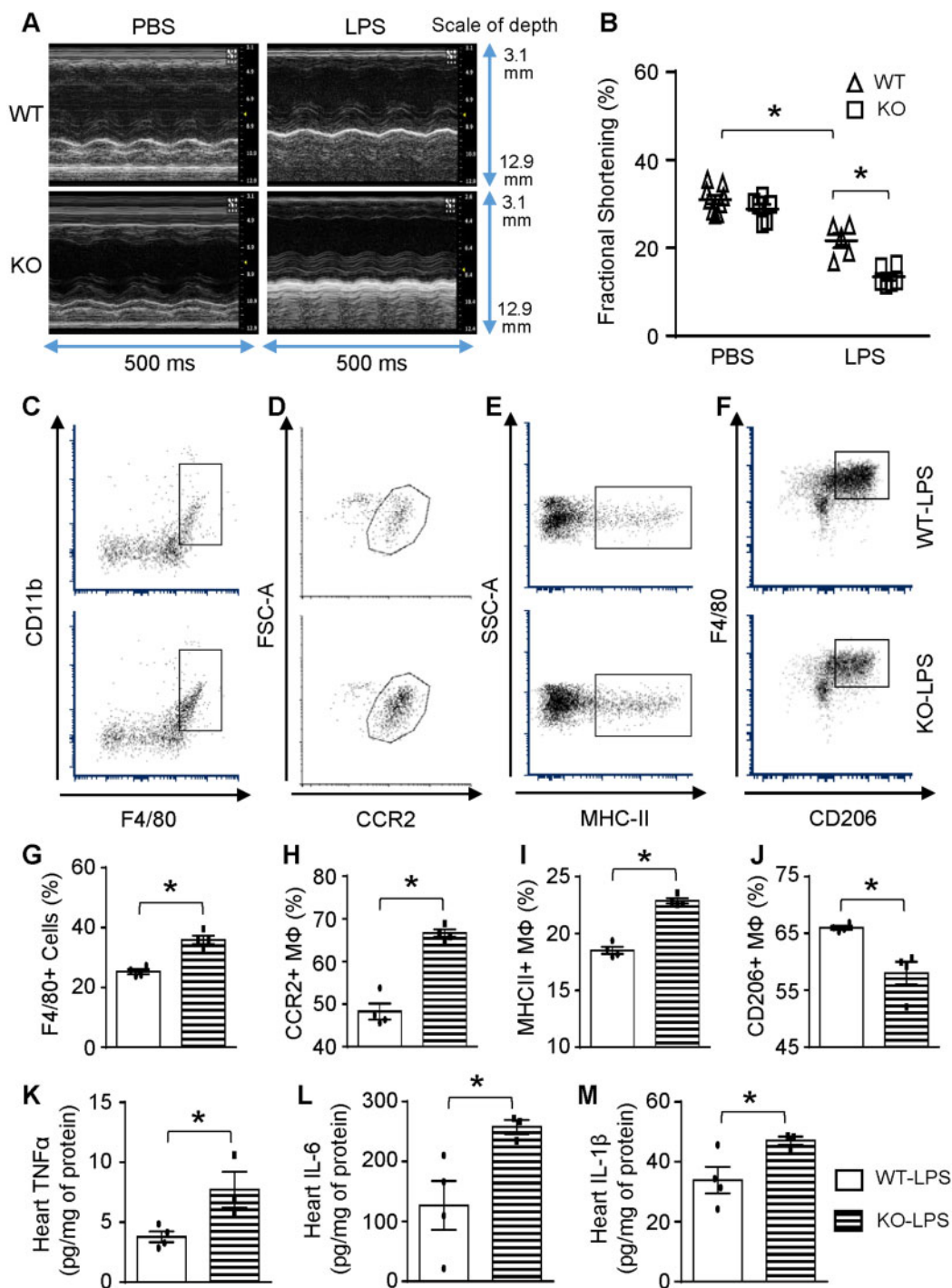


**Figure 3** Sectm1a deficiency enhances cardiac inflammation and dysfunction. 12 h after injecting mice with LPS (10 mg/kg) (A and B) cardiac function was determined by echocardiography ( $n = 5-9$ ). (C-J) Representative flow cytometry plots and quantification of cardiac macrophage marker expression showed more macrophage accumulation (F4/80+) with inflammatory phenotype (CCR2+, MHC-II+, CD206-) in the heart of KO mice 12 h after LPS injection ( $n = 4$ ). Gating strategy is shown in [Supplementary material online, Figure S3A](#). (K-M) cytokine levels in the myocardium were measured by ELISA ( $n = 3-4$ ) (\* $P < 0.05$ ; data are presented as mean  $\pm$  SEM; Student's  $t$ -test).

macrophages, while LXR $\beta$  levels exhibited no difference between two groups ([Supplementary material online, Figure S5B](#)). Further analysis revealed that 100 LXR-related genes were differentially expressed in Sectm1a-KO BMDMs ([Figure 5E](#)). Consistent with the RNA-seq data,

qRT-PCR validated significant decreases in the expression of several noted LXR-targeted genes: ApoE, ABCA1, ABCG1, CD36, and MMP12 ([Figure 5F](#)). Taken together, these data suggest that absence of Sectm1a could impair LXR $\alpha$  signal in macrophages.

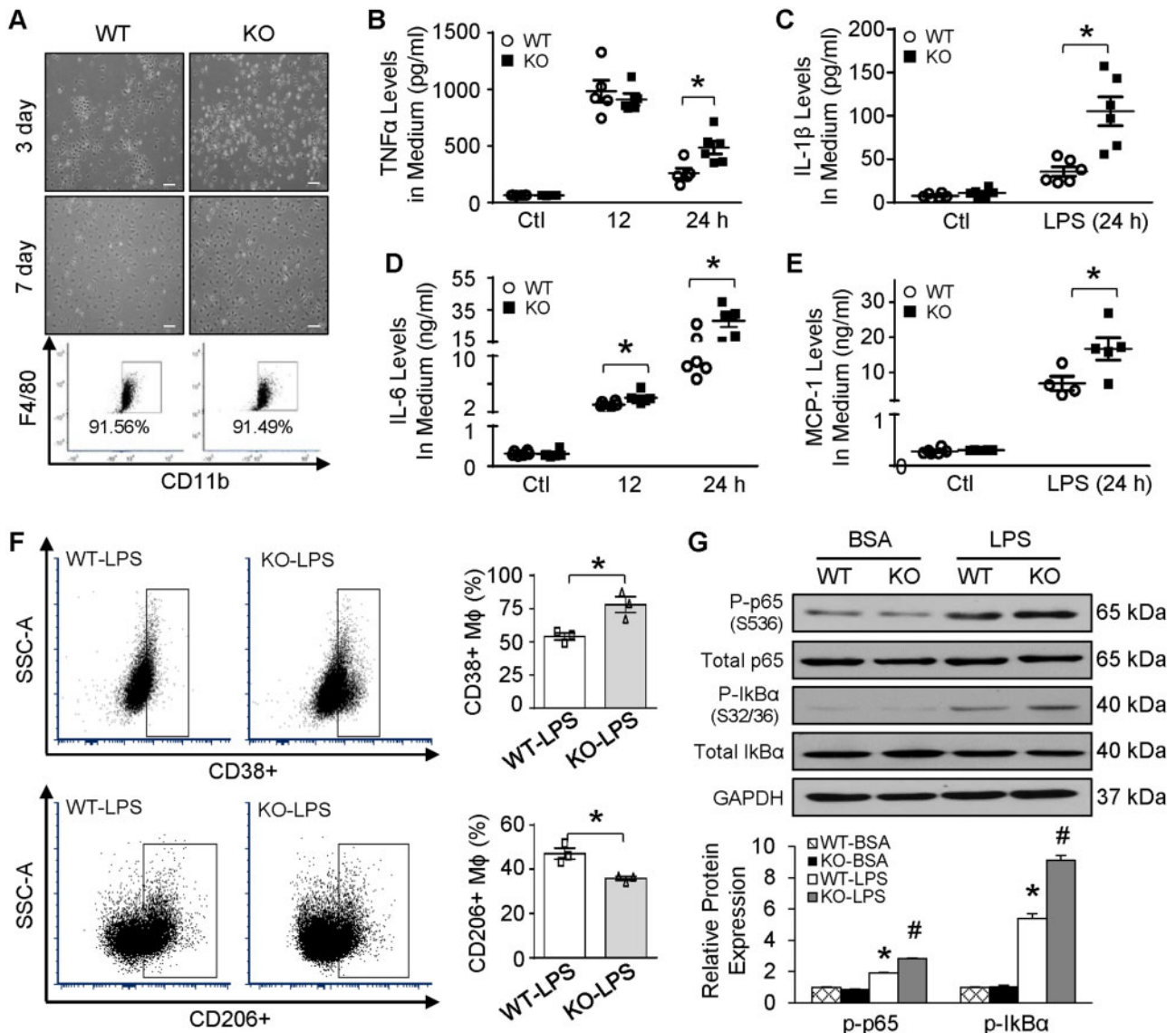


**Figure 4** Lack of Sectm1a augments LPS-induced inflammation via skewing BMDMs towards pro-inflammatory phenotype. BMDMs were isolated from WT and Sectm1a KO mice allowed to differentiate for 7 days (A) representative images of mature BMDMs and flow cytometry analyses showed no differences on cell morphology and differentiation. (B–E) After treating BMDMs with LPS (10 ng/mL), cytokine levels: TNF $\alpha$  (B), IL-1 $\beta$  (C), IL-6 (D), and MCP-1 (E) from cell culture supernatant were measured using ELISA at 12- and 24-h time points ( $n = 4-6$ ). (F) Representative flow cytometry plots and quantification of macrophage marker expression revealed stronger inflammatory phenotype, as evidenced by increased CD38+ and lowered CD206+ expression, in KO BMDMs 6 h after LPS treatment ( $n = 3$  dishes of BMDMs, each from separate mouse). (G) Western blotting of phosphorylated p65 and I $\kappa$ B $\alpha$  in BMDMs with or without LPS stimulation (10 ng/mL, 30 min.) ( $n = 3$  dishes of BMDMs for isolation of proteins, each dish from separate mouse) (Scale bar, 200  $\mu$ m; \* $P < 0.05$ ; #  $P < 0.05$  when comparing WT-LPS to KO-LPS; data are presented as mean  $\pm$  SEM; Student's *t*-test).

### 3.6 LXR agonist fails to rescue LPS-induced inflammation and cardiac dysfunction in Sectm1a-KO model

To assess how LXR $\alpha$  signalling is modulated in Sectm1a-KO BMDMs upon LPS challenge, we performed qRT-PCR to determine the gene expression of LXR $\alpha$  and its downstream targets. After treating BMDMs with LPS for 3 h, expression levels of LXR $\alpha$  and ABCG1 were significantly reduced in WT-LPS group, when compared with WT-PBS group (Figure 6A). Importantly, when comparing with WT-BMDMs after LPS

treatment, the mRNA levels of LXR $\alpha$ , ABCA1, ABCG1, and ApoE were further decreased in KO-LPS group (Figure 6A). These data suggest that Sectm1a deficiency aggravates LPS-mediated suppression of LXR $\alpha$  signalling cascade in macrophages. Given that LXR $\alpha$  contributes to Sectm1a-induced action in macrophages response to LPS stimulation, we next treated WT- and KO-BMDMs with GW3965, a potent LXR agonist, 12 h prior to LPS stimulation, for determining whether Sectm1a deficiency affects LXR signalling (Figure 6B). As expected, treatment of GW3965 markedly increased the nuclear translocation of LXR $\alpha$  when

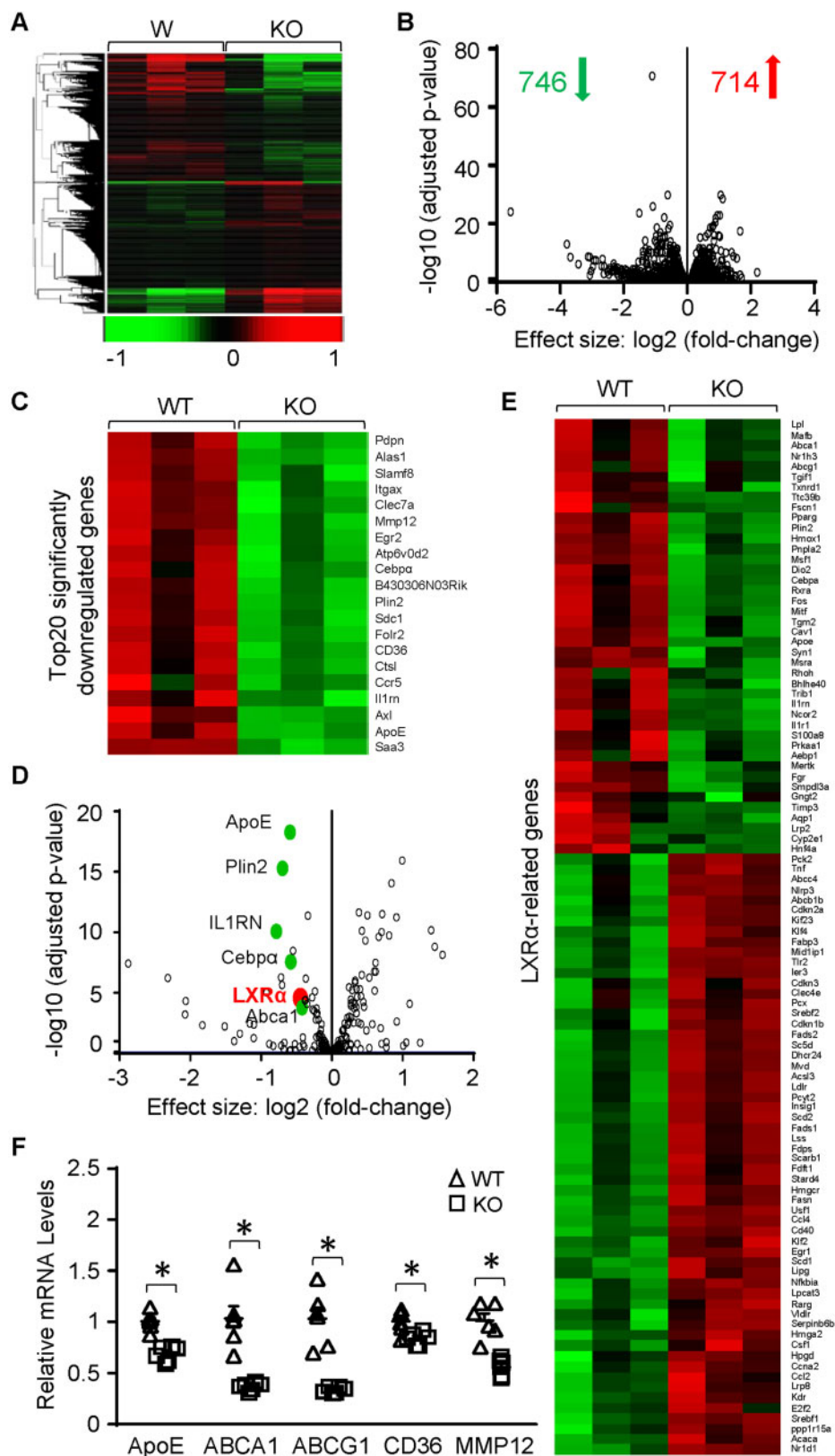


**Figure 5** Gene expression profile in Sctm1a KO BMDMs determined by high-throughput RNA-seq. (A and B) Heatmap (A) and volcano plot (B) of the overall gene expression alteration in BMDMs isolated from WT and Sctm1a KO mice ( $n = 3$  per genotype). (C) Heatmap showing the top 20 most significantly down-regulated genes in Sctm1a KO BMDMs. (D and E) Volcano plot (D) and heat-map (E) of all LXR-related genes that were differentially expressed in Sctm1a KO BMDMs. (F) expression of most common LXR-target genes in Sctm1a KO BMDMs were validated using qRT-PCR.  $n = 3$  for each genotype (\* $P < 0.05$ ; data are presented as mean  $\pm$  SEM; Student's  $t$ -test).



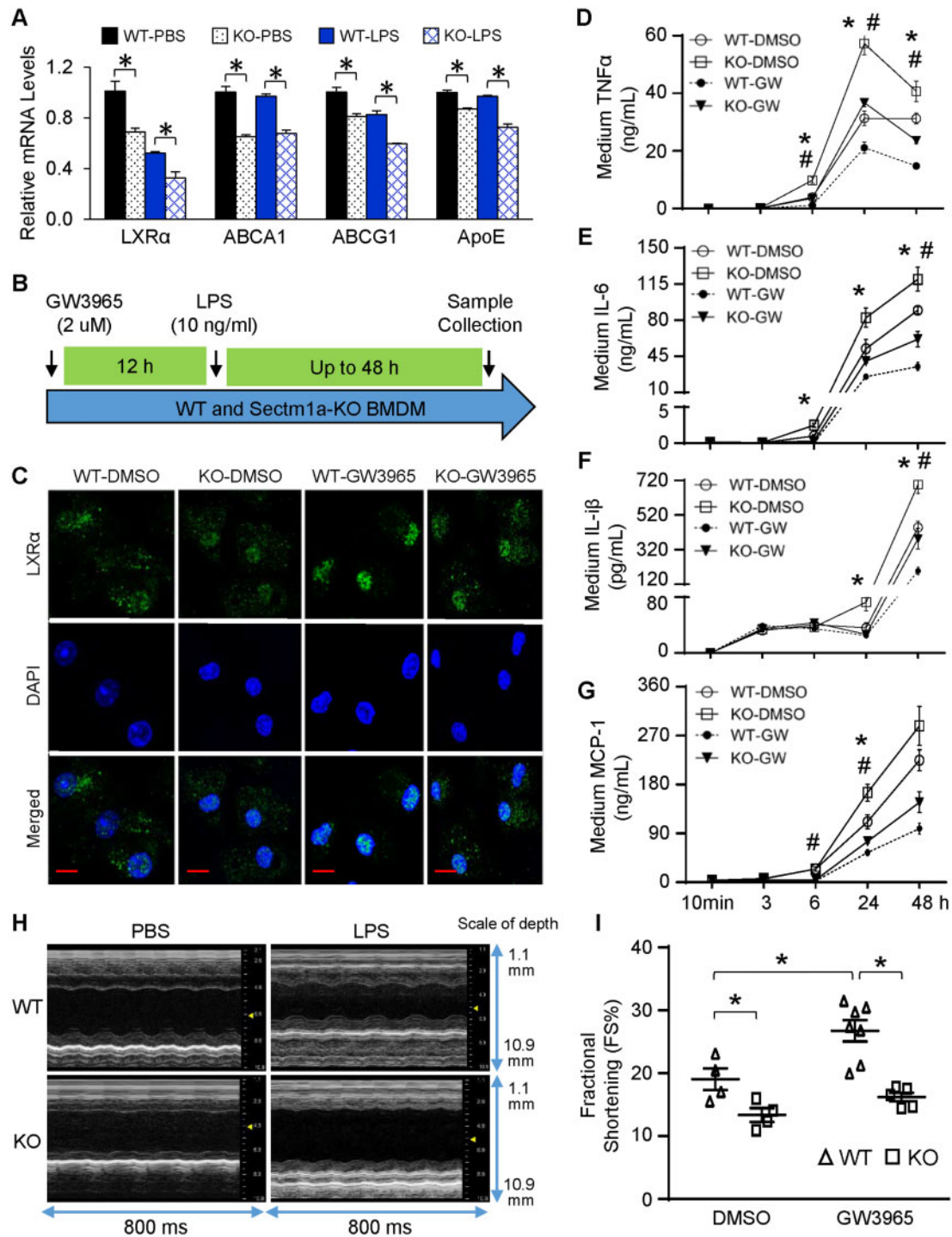


**Figure 6** LXR agonist fails to rescue LPS-induced inflammation and cardiac dysfunction in Sectm1a KO model. (A) Gene expression of LXR $\alpha$  and target genes in WT and Sectm1a-KO BMDMs after 3 h of LPS (10 ng/mL) treatment was measured using qRT-PCR ( $n = 3$ ). (B) Graphic scheme of treatment protocol. BMDMs from WT and Sectm1a KO mice were first treated with LXR agonist, GW3965 (2  $\mu$ m, 12 h) followed by LPS stimulation (10 mg/mL, up to 48 h). (C) Immunofluorescent staining of BMDMs with LXR $\alpha$  after 12 h GW3965 and 30 min LPS treatment. DNA was stained with DAPI (blue). (D–G) After treating BMDMs with GW3965 for 12 h, cytokine levels in cell culture supernatant was determined by ELISA at indicated time points post-LPS treatment ( $n = 4–5$ ). (H and I) WT and Sectm1a KO mice received three injections of GW3965 (30 mg/kg of BW, once daily, DMSO used as control), 6 h after last GW3965 injection, all mice received LPS injection (10 mg/kg) and underwent echocardiography measurement to assess cardiac function ( $n = 4–7$ ) (Scale bar, 10  $\mu$ m; \* $P < 0.05$  when comparing WT-DMSO to WT-GW, # $P < 0.05$  when comparing WT-GW to KO-GW; data are presented as mean  $\pm$  SEM; two-way ANOVA).

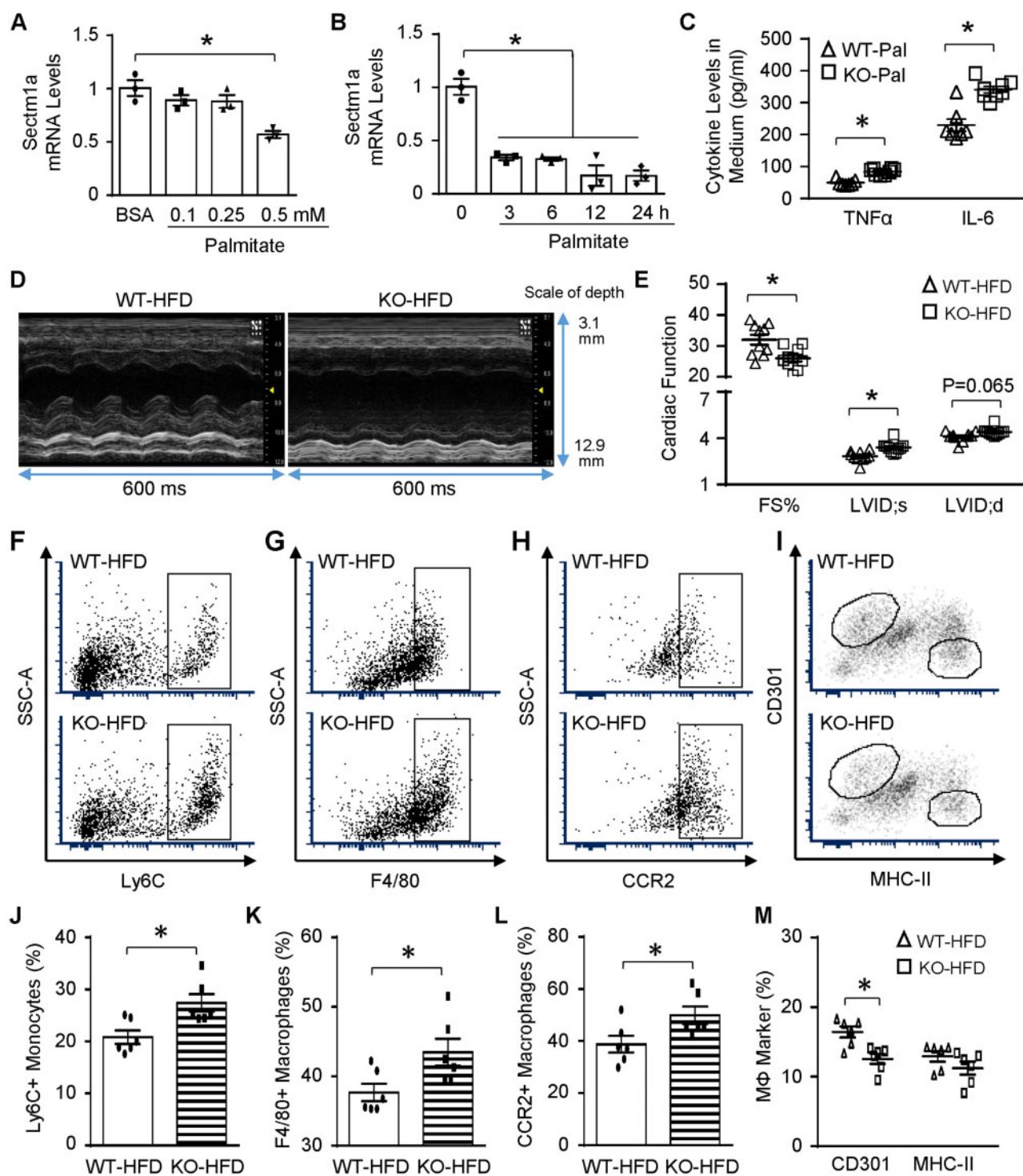


**Figure 7** Lack of Sectm1a promotes HFD-induced cardiac inflammation and dysfunction. (A) WT BMDMs were treated with indicated doses of palmitate for 24 h and (B) RAW264.7 macrophages were treated with 0.5 mM palmitate for indicated time points, then gene expression of Sectm1a was measured with qRT-PCR ( $n=3$ ). (C) WT and Sectm1a KO BMDMs were treated with palmitate (0.5 mM, 24 h), and cytokine levels in cell culture supernatant were measured using ELISA ( $n=7-8$ ). (D and E) Cardiac function was determined by echocardiography after WT and Sectm1a KO mice were fed with HFD for 20 weeks ( $n=10$  per group). (F–M) Representative flow cytometry plots and quantification of cardiac macrophage marker expression showed more monocytes (Ly6C $^{+}$ ) and macrophage accumulation (F4/80 $^{+}$ ) with inflammatory phenotype (CCR2 $^{+}$ , CD301 $^{-}$ ) in the heart of KO mice 5 weeks after HFD feeding ( $n=6$ ). FS, fractional shortening; LVID;d, left ventricular internal diameter at diastole; LVID;s, left ventricular internal diameter at systole (\* $P < 0.05$ ; data are presented as mean  $\pm$  SEM; Student's  $t$ -test).

comparing WT-GW3965 to WT-BSA group (Figure 6C), and resulted in substantial reduction of pro-inflammatory factor (TNF $\alpha$ , IL-6, IL-1 $\beta$ , and MCP-1) secretion as early as 6 h after LPS treatment (Figure 6D–G). In contrast, treatment of Sectm1a-KO BMDMs with GW3965 showed that more LXR $\alpha$  was retained in the cytosol than WT-GW3965 control cells (Figure 6C). Accordingly, the concentration of pro-inflammatory factors was significantly higher in cell culture supernatants of KO-GW3965 macrophages than WT-GW3965 group upon LPS treatment (Figure 6D–G). Previous studies have reported the cardiac protective effects of GW3965 in db/db diabetic and ischaemic/reperfused mouse models, which is mainly mediated through LXR $\alpha$  instead of LXR $\beta$  subtype.<sup>40,41</sup> Consistently, we here showed that LPS-induced cardiac dysfunction was improved with GW3965 injection, evidenced by 29% increase in fractional shortening (FS %) when compared with WT-DMSO group (Figure 6H and I and Supplementary material online, Table S2). However, such protective effect was diminished in Sectm1a-KO mice, as the percentage of fractional shortening showed no difference between KO-DMSO and KO-GW3965 groups (Figure 6H and I, Supplementary material online, Table S2). Taken together, these results indicate that Sectm1a KO-mediated inflammatory responses in macrophages may be ascribed to the disruption of LXR $\alpha$  pathway, and subsequently fail to improve cardiac function after treatment of LXR agonist.

### 3.7 Sectm1a-KO provokes HFD-induced inflammation and cardiac dysfunction

Given the pivotal roles of Sectm1a in regulating acute inflammatory response in mice with endotoxaemia, we were interested in exploring whether Sectm1a is also involved in chronic inflammatory conditions (i.e. obesity). After treating WT-BMDMs with palmitate for 24 h, we observed significant (43%) reduction in Sectm1a gene expression only at 0.5 mM dose (Figure 7A). Of interest, by using the same dose, Sectm1a level was down-regulated in RAW264.7 macrophages as early as 3 h after palmitate treatment (Figure 7B). To determine whether Sectm1a may affect macrophage activation upon lipid stimulation, BMDMs from WT- and Sectm1a-KO mice were treated with 0.5 mM palmitate for 24 h. The results showed significantly higher levels of TNF $\alpha$  and IL-6 in KO-palmitate group, when compared with WT-palmitate control (Figure 7C). Consistent with above acute inflammation model, cardiac function was suppressed in Sectm1a-KO mice, compared to WT controls, after 20-wk HFD feeding (Figure 7D and E, and Supplementary material online, Table S3). This phenomenon may be at least partially caused by: (i) increased infiltration of monocytes (Ly6C+) and macrophages (F4/80+) with higher expression of CCR2, an inflammatory marker, into KO-HFD hearts (Figure 7F–H, J–L); and (ii) reduced levels of anti-inflammatory marker, CD301, on cardiac macrophages isolated from KO-HFD mice (Figure 7I/M). Put together, these data indicate that Sectm1a deficiency is also involved in chronic inflammatory responses and causes cardiac dysfunction under HFD-induced obese condition.

## 4. Discussion

In the present study, we have identified Sectm1a as a previously unrecognized regulator of inflammatory responses, specifically macrophage activation, both during endotoxaemia (LPS-induced acute inflammation) and upon HFD feeding (similar to chronic low-grade inflammation observed in obese population). Sectm1a KO mice that were injected with LPS or fed a HFD showed greater propensity for enhanced inflammatory responses and cardiac dysfunction than that of WT control groups.

Macrophages with Sectm1a deficiency were skewed towards inflammatory phenotype with increased secretion of inflammatory cytokines, which are key mediators of cardiac dysfunction. Using high-throughput RNA-sequencing, we have identified that the LXR $\alpha$  signalling pathway was disrupted in macrophages due to lack of Sectm1a; and treatment of macrophages with LXR agonist, GW3965, did not suppress cytokine release and failed to rescue cardiac function when comparing Sectm1a KO group to the WT counterparts. Collectively, these findings uncover the critical role of Sectm1a in the regulation of endotoxin- and obesity-associated inflammation and cardiac dysfunction.

In this study, we found that Sectm1a was greatly down-regulated in BMDMs at the later phase of LPS (24–48 h post-LPS, Figure 1B) or palmitate treatments (Figure 7B). Our findings are consistent with previous studies showing that human Sectm1 is an early response gene to IFN $\gamma$  in MM6 human monocytes, where its expression is increased at early time points (3, 6, 12 h) but decreases after 24 h; and the induction of Sectm1 expression by IFN $\gamma$  can be suppressed by LPS.<sup>30</sup> Here, we showed that Sectm1a expression was increased by more than 900-fold in WT BMDMs 4 h after IFN $\gamma$  (10 ng/mL) treatment, but when BMDMs were treated with IFN $\gamma$  and LPS, expression of Sectm1a was only increased by 20-fold (Supplementary material online, Figure S6). Interestingly, TNF $\alpha$  mRNA levels were 10-fold higher in IFN $\gamma$ +LPS group when comparing to IFN $\gamma$  alone group (Supplementary material online, Figure S6), indicating that LPS-induced reduction of Sectm1a expression was able to trigger stronger inflammatory response. Indeed, Tsalik et al.<sup>42</sup> recently sequenced peripheral blood RNA of 129 representative subjects with systemic inflammatory response syndrome (SIRS) or sepsis including 78 sepsis survivors and 28 sepsis non-survivors, and revealed that Sectm1 was significantly higher in sepsis survivors, compared to non-survivor SIRS controls. On the other hand, Sectm1b was previously reported to inhibit T-cell activation.<sup>28</sup> However, given that Sectm1b shares less than 40% protein homology with either Sectm1a or human Sectm1<sup>28</sup>; the expression levels of Sectm1b in BMDMs showed no difference after LPS treatment (Supplementary material online, Figure S1C); and ablation of Sectm1a does not affect Sectm1b expression (Supplementary material online, Figure S2), we speculate that Sectm1b might not participate in the regulation of macrophage activation. Collectively, these findings suggest that Sectm1a may act as an anti-inflammatory mediator, and its expression could be promptly reduced as inflammatory response progresses.

Following an insult by either intrinsic or extrinsic stimuli, the interplay of cardiomyocytes, cardiac fibroblasts, and innate immune cells determine an effective recovery or insufficient repair of damaged tissue. Macrophages, as the most abundant leucocytes in the heart, comprise 5–10% of total nonmyocytes with great heterogeneity in origin.<sup>43</sup> In particular, abundance and phenotype of macrophages are altered during inflammatory and reparative processes.<sup>37,43</sup> Recent studies reveal that, similar to mouse hearts, human cardiac macrophages can also be partitioned into distinct subsets depending on the expression of CCR2, a critical factor required for monocyte migration. As demonstrated by various approaches including genetic fate mapping, single-cell transcriptomics, and parabiosis, cardiac CCR2-macrophages are a self-maintained resident population established early in development; whereas CCR2+ macrophages are derived from recruited monocytes and replenished through proliferation.<sup>44,45</sup> More importantly, CCR2+ macrophages are critical players to co-ordinate cardiac inflammation with marked increase of IL-1 $\beta$ ; and the change of absolute number or percentage of CCR2+ macrophages is positively correlated with left ventricular systolic dysfunction following mechanic unloading.<sup>43</sup> Consistently, our findings showed substantial increased of CCR2+ macrophages in the hearts of

Sectm1a KO mice with LPS injection or HFD feeding, resulting in exacerbated inflammation and cardiac suppression. Accordingly, Sectm1a-deficient macrophages released profoundly higher levels of cytokines (TNF $\alpha$ , IL-6, and IL1 $\beta$ ), which are well-known inflammatory mediators that are ascribed to the pathogenesis of heart failure.<sup>46,47</sup> In particular, IL-6 was the most abundant cytokine in the myocardium of WT mouse after LPS injection, yet the concentration of IL-6 protein was 2-fold higher in Sectm1a KO mouse hearts, when compared with WT-LPS group (Figure 3K–M), which suggested that IL-6 may be the major contributor to cardiac dysfunction in Sectm1a KO mice under inflammatory condition. In contrast, when Sectm1a was overexpressed in BMDMs using adenovirus (Ad.Sectm1a), production of inflammatory cytokines after LPS treatment was significantly lower in Ad.Sectm1a group than Ad.GFP control group. However, we did not detect such anti-inflammatory effects from Sectm1a overexpression in cardiomyocytes (Supplementary material online, Figure S4), suggesting that the observed inflammatory phenotype was mainly contributed by macrophages instead of cardiomyocytes.

Along this line, as instructed by the RNA-Sequencing analyses, we provide further insight into Sectm1a-mediated regulation of macrophage activation through LXR signalling pathway. We observed that Sectm1a deficiency had dramatically increased inflammatory response and aggravated cardiac dysfunction, when stimulated with LPS, which cannot be rescued by treatment with LXR agonist. Mechanistically, LXR $\alpha$  has been demonstrated to regulate NF- $\kappa$ B pathway, and thereby controls the downstream inflammatory responses in macrophages.<sup>21,22</sup> Consistently, when LXR $\alpha$  gene expression and activation was suppressed in WT BMDMs treated with LPS (Figure 6A), we observed increased phosphorylation of p65 and I $\kappa$ B $\alpha$  (Figure 4G), indicating activated NF- $\kappa$ B pathway. Importantly, when comparing to WT-LPS group, Sectm1a deficiency further suppressed LXR $\alpha$  signalling cascade, resulting in augmented phosphorylation of p65 and I $\kappa$ B $\alpha$ . However, activation of NF- $\kappa$ B pathway could be alleviated by overexpressing Sectm1a in BMDMs and led to lower production of inflammatory cytokines (Supplementary material online, Figure S4A–G). These data collectively suggest that Sectm1a could suppress inflammatory response by inhibiting NF- $\kappa$ B signalling through activation of LXR $\alpha$  pathway. Nonetheless, more detailed experiments are needed to unravel how Sectm1a regulates LXR pathway, and future studies focusing on dissecting the protein structure of Sectm1a and its interaction to LXR $\alpha$  should be warranted. Furthermore, subsequent gene network analysis identified that three genes (IL-1RN, Cav1, S100a8) were involved in sepsis, cardiovascular diseases and LXR signalling cascade, and IL-1RN showed highest expression with most significant reduction (Supplementary material online, Figure S5C and D). Future investigation exploring the effects of IL-1RN might be beneficial to clarify the mechanism of Sectm1a.

In conclusion, our study presented here for the first time utilizes a KO mouse model, and clearly demonstrates that, through disrupted LXR signalling pathway, Sectm1a deficiency robustly provokes LPS- and HFD-induced inflammation, as evidenced by higher levels of inflammatory cytokines both *in vivo* (plasma and myocardium) and *in vitro* (BMDMs), as well as increased infiltration of macrophages to the heart, leading to aggravated suppression of cardiac contractility. Therefore, approaches that enhance Sectm1a expression/activity would possess great therapeutic potential to treat inflammatory disease and its associated cardiac dysfunction.

## Supplementary material

Supplementary material is available at *Cardiovascular Research* online.

## Authors' contributions

Y.L. designed, performed experiments, analysed data, and wrote and edited the manuscript. S.D., X.W., X.M., and K.E. assisted with various experiments (particularly flow cytometry) and helped with analysing data. W.H., N.R., J.R., and Y.W. performed, analysed and provide guidance on echocardiography. J.C. and A.J. analysed RNA-sequencing data. T.P. and D.A. helped with experimental design, data analysis and revised the manuscript. J.P. and G.F. supervised and conceptualized the study and edited the manuscript.

**Conflict of interest:** none declared.

## Funding

This work was supported by American Heart Association (AHA) Established Investigator Award [17EIA33400063 to G.-C.F.], National Institute of Health [GM-126061 and GM-132149 to G.-C.F.], AHA Pre-doctoral Fellowship [18PRE33960576 to Y.L.].

## References

- Medzhitov R, Horng T. Transcriptional control of the inflammatory response. *Nat Rev Immunol* 2009;**10**:692–703.
- Prasad S, Aggarwal BB. Chronic diseases caused by chronic inflammation require chronic treatment: anti-inflammatory role of dietary spices. *J Clin Cell Immunol* 2014;**05**:238.
- Wassenaar TM, Zimmermann K. Lipopolysaccharides in food, food supplements, and probiotics: should we be worried? *Eur J Microbiol Immunol (Bp)* 2018;**3**:63–69.
- van Lier D, Geven C, Leijte GP, Pickkers P. Experimental human endotoxemia as a model of systemic inflammation. *Biochimie* 2019;**159**:99–106.
- Lumeng CN, Sattiel AR. Inflammatory links between obesity and metabolic disease. *J Clin Invest* 2011;**121**:2111–2117.
- Bonacina F, Moregola A, Porte R, Baragetti A, Bonavita E, Salatin A, Grigore L, Pellegatta F, Molgora M, Sironi M, Barbati E, Mantovani A, Bottazzi B, Catapano AL, Garlanda C, Norata GD. Pentraxin 3 deficiency protects from the metabolic inflammation associated to diet-induced obesity. *Cardiovasc Res* 2019;**115**:1861–1872.
- Havaldar AA. Evaluation of sepsis induced cardiac dysfunction as a predictor of mortality. *Cardiovasc Ultrasound* 2018;**16**:31.
- Jeong HS, Lee TH, Bang CH, Kim JH, Hong SJ. Risk factors and outcomes of sepsis-induced myocardial dysfunction and stress-induced cardiomyopathy in sepsis or septic shock: a comparative retrospective study. *Medicine (Baltimore)* 2018;**97**:e0263.
- Kenchaiah S, Evans JC, Levy D, Wilson PW, Benjamin EJ, Larson MG, Kannel WB, Vasan RS. Obesity and the risk of heart failure. *N Engl J Med* 2002;**347**:305–313.
- Alpert MA, Lavie CJ, Agrawal H, Aggarwal KB, Kumar SA. Obesity and heart failure: epidemiology, pathophysiology, clinical manifestations, and management. *Transl Res* 2014;**164**:345–356.
- Rech M, Barandiarán Aizpurua A, van Empel V, van Bilsen M, Schroen B. Pathophysiological understanding of HFpEF: microRNAs as part of the puzzle. *Cardiovasc Res* 2018;**114**:782–793.
- Liu YC, Yu MM, Shou ST, Chai YF. Sepsis-induced cardiomyopathy: mechanisms and treatments. *Front Immunol* 2017;**8**:1021.
- Ziegler KA, Ahles A, Wille T, Kerler J, Ramanujam D, Engelhardt S. Local sympathetic denervation attenuates myocardial inflammation and improves cardiac function after myocardial infarction in mice. *Cardiovasc Res* 2018;**114**:291–299.
- Swirski FK, Pittet MJ, Kircher MF, Aikawa E, Jaffer FA, Libby P, Weissleder R. Monocyte accumulation in mouse atherogenesis is progressive and proportional to extent of disease. *Proc Natl Acad Sci USA* 2006;**103**:10340–10345.
- Bobryshev YV, Ivanova EA, Chistiakov DA, Nikiforov NG, Orekhov AN. Macrophages and their role in atherosclerosis: pathophysiology and transcriptome analysis. *Biomed Res Int* 2016;**2016**:9582430.
- Huang P, Chandra V, Rastinejad F. Structural overview of the nuclear receptor superfamily: insights into physiology and therapeutics. *Annu Rev Physiol* 2010;**72**:247–272.
- Wang K, Wan YJ. Nuclear receptors and inflammatory diseases. *Exp Biol Med (Maywood)* 2008;**233**:496–506.
- Joseph SB, Castrillo A, Laffitte BA, Mangelsdorf DJ, Tontonoz P. Reciprocal regulation of inflammation and lipid metabolism by liver X receptors. *Nat Med* 2003;**9**:213–219.
- Per-Arne S, Daniel AH, Margareta J, Mikael COE, Lillemor MH, Bertil GO, Johannes H, Olov W, Bjorn C, Bjorn F, Lena MSC. Identification of genes predominantly expressed in human macrophages. *Atherosclerosis* 2004;**2**:287–290.
- Botez G, Piraino G, Hake PW, Ledford JR, O'Connor M, Cook JA, Zingarelli B. Age-dependent therapeutic effects of liver X receptor- $\alpha$  activation in murine polymicrobial sepsis. *Innate Immun* 2015;**21**:609–618.

21. Wu S, Yin R, Ernest R, Li Y, Zhelyabovska O, Luo J, Yang Y, Yang Q. Liver X receptors are negative regulators of cardiac hypertrophy via suppressing NF-kappaB signaling. *Cardiovasc Res* 2009;**84**:19–126.
22. Ito A, Hong C, Rong X, Zhu X, Tarling EJ, Hedde PN, Gratton E, Parks J, Tontonoz P. LXRs link metabolism to inflammation through Abca1-dependent regulation of membrane composition and TLR signaling. *Elife* 2015;**4**:e08009.
23. Castrillo A, Joseph SB, Vaidya SA, Haberland M, Fogelman AM, Cheng G, Tontonoz P. Crosstalk between LXR and toll-like receptor signaling mediates bacterial and viral antagonism of cholesterol metabolism. *Mol Cell* 2003;**12**:805–816.
24. Matalonga J, Glaria E, Bresque M, Escande C, Carbó JM, Kiefer K, Vicente R, León TE, Beceiro S, Pascual-García M, Serret J, Sanjurjo L, Morón-Ros S, Riera A, Paytubi S, Juarez A, Sotillo F, Lindbom L, Caelles C, Sarrías MR, Sancho J, Castrillo A, Chini EN, Valledor AF. The nuclear receptor LXR limits bacterial infection of host macrophages through a mechanism that impacts cellular NAD metabolism. *Cell Rep* 2017;**18**:1241–1255.
25. Joseph SB, Bradley MN, Castrillo A, Bruhn KW, Mak PA, Pei L, Hogenesch J, O'Connell RM, Cheng G, Saez E, Miller JF, Tontonoz P. LXR-dependent gene expression is important for macrophage survival and the innate immune response. *Cell* 2004;**119**:299–309.
26. Slentz-Kesler KA, Hale LP, Kaufman RE. Identification and characterization of K12 (SECTM1), a novel human gene that encodes a Golgi-associated protein with transmembrane and secreted isoforms. *Genomics* 1998;**47**:327–340.
27. Kamata H, Yamamoto K, Wasserman GA, Zabinski MC, Yuen CK, Lung WY, Gower AC, Belkina AC, Ramirez MI, Deng JC, Quinton LJ, Jones MR, Mizgerd JP. Epithelial cell-derived secreted and transmembrane 1a signals to activated neutrophils during pneumococcal pneumonia. *Am J Respir Cell Mol Biol* 2016;**55**:407–418.
28. Howie D, Garcia Rueda H, Brown MH, Waldmann H. Secreted and transmembrane 1A is a novel co-stimulatory ligand. *PLoS One* 2013;**8**:e73610.
29. Wang T, Ge Y, Xiao M, Lopez-Coral A, Li L, Roesch A, Huang C, Alexander P, Vogt T, Xu X, Hwang WT, Lieu M, Belsler E, Liu R, Somasundaram R, Herlyn M, Kaufman RE. SECTM1 produced by tumor cells attracts human monocytes via CD7-mediated activation of the PI3K pathway. *J Invest Dermatol* 2014;**134**:1108–1118.
30. Huyton T, Göttmann W, Bade-Döding C, Paine A, Blaszczk R. The T/NK cell costimulatory molecule SECTM1 is an IFN "early response gene" that is negatively regulated by LPS in human monocyte cells. *Biochim Biophys Acta* 2011;**1810**:1294–1301.
31. Trouplin V, Boucherit N, Gorvel L, Conti F, Mottola G, Ghigo E. Bone marrow-derived macrophage production. *J Vis Exp* 2013;**81**:e50966.
32. Wang L, Li Y, Wang X, Wang P, Essandoh K, Cui S, Huang W, Mu X, Liu Z, Wang Y, Peng T, Fan GC. GDF3 protects mice against sepsis-induced cardiac dysfunction and mortality by suppression of macrophage pro-inflammatory phenotype. *Cells* 2020;**9**:e120.
33. Qin D, Wang X, Li Y, Wang L, Wang R, Peng J, Essandoh K, Mu X, Peng T, Han Q, Yu KJ, Fan GC. MicroRNA-223-5p and -3p cooperatively suppress necroptosis in ischemic/reperfused hearts. *J Biol Chem* 2016;**291**:20247–20259.
34. Wang X, Gu H, Huang W, Peng J, Li Y, Yang L, Qin D, Essandoh K, Wang Y, Peng T, Fan GC. Hsp20-mediated activation of exosome biogenesis in cardiomyocytes improves cardiac function and angiogenesis in diabetic mice. *Diabetes* 2016;**65**:3111–3128.
35. Yu YR, O'Koren EG, Hotten DF, Kan MJ, Kopin D, Nelson ER, Que L, Gunn MD. A protocol for the comprehensive flow cytometric analysis of immune cells in normal and inflamed murine non-lymphoid tissues. *PLoS One* 2016;**11**:e0150606.
36. Peng J, Li Y, Wang X, Deng S, Holland J, Yates E, Chen J, Gu H, Essandoh K, Mu X, Wang B, McNamara RK, Peng T, Jegga AG, Liu T, Nakamura T, Huang K, Perez-Tilve D, Fan GC. An Hsp20-FBXO4 axis regulates adipocyte function through modulating PPAR $\gamma$  ubiquitination. *Cell Rep* 2018;**23**:3607–3620.
37. Ma Y, Mouton AJ, Lindsey ML. Cardiac macrophage biology in the steady-state heart, the aging heart, and following myocardial infarction. *Transl Res* 2018;**191**:15–28.
38. Christian F, Smith EL, Carmody RJ. The regulation of NF-kB subunits by phosphorylation. *Cells* 2016;**5**:e12.
39. Wang Y, Liu J, Kong Q, Cheng H, Tu F, Yu P, Liu Y, Zhang X, Li C, Li Y, Min X, Du S, Ding Z, Liu L. Cardiomyocyte-specific deficiency of HSPB1 worsens cardiac dysfunction by activating NFkB-mediated leucocyte recruitment after myocardial infarction. *Cardiovasc Res* 2019;**115**:154–167.
40. He Q, Pu J, Yuan A, Yao T, Ying X, Zhao Y, Xu L, Tong H, He B. Liver X receptor agonist treatment attenuates cardiac dysfunction in type 2 diabetic db/db mice. *Cardiovasc Diabetol* 2014;**13**:149.
41. He Q, Pu J, Yuan A, Lau WB, Gao E, Koch WJ, Ma XL, He B. Activation of liver-X-receptor  $\alpha$  but not liver-X-receptor  $\beta$  protects against myocardial ischemia/reperfusion injury. *Circ Heart Fail* 2014;**7**:1032–1041.
42. Tsalik EL, Langley RJ, Dinwiddie DL, Miller NA, Yoo B, van Velkinburgh JC, Smith LD, Thiffault I, Jaehne AK, Valente AM, Henao R, Yuan X, Glickman SW, Rice BJ, McClain MT, Carin L, Corey GR, Ginsburg GS, Cairns CB, Otero RM, Fowler VG Jr, Rivers EP, Woods CW, Kingsmore SF. An integrated transcriptome and expressed variant analysis of sepsis survival and death. *Genome Med* 2014;**6**:e111.
43. Pinto AR, Ilinykh A, Ivey MJ, Kuwabara JT, D'Antoni ML, Debuque R, Chandran A, Wang L, Arora K, Rosenthal NA, Tallquist MD. Revisiting cardiac cellular composition. *Circ Res* 2016;**118**:400–409.
44. Andreadou I, Cabrera-Fuentes HA, Devaux Y, Frangogiannis NG, Frantz S, Guzik T, Liehn EA, Gomes CPC, Schulz R, Hausenloy DJ. Immune cells as targets for cardioprotection: new players and novel therapeutic opportunities. *Cardiovasc Res* 2019;**115**:1117–1130.
45. Bajpai G, Schneider C, Wong N, Bredemeyer A, Hulsmans M, Nahrendorf M, Epelman S, Kreisler D, Liu Y, Itoh A, Shankar TS, Selzman CH, Drakos SG, Lavine KJ. The human heart contains distinct macrophage subsets with divergent origins and functions. *Nat Med* 2018;**24**:1234–1245.
46. Zhang Y, Huang Z, Li H. Insights into innate immune signalling in controlling cardiac remodelling. *Cardiovasc Res* 2017;**113**:1538–1550.
47. Zuurbier CJ, Abbate A, Cabrera-Fuentes HA, Cohen MV, Collino M, De Kleijn DPV, Downey JM, Pagliaro P, Preissner KT, Takahashi M, Davidson SM. Innate immunity as a target for acute cardioprotection. *Cardiovasc Res* 2019;**115**:1131–1142.

## Translational perspective

Better understanding on the interaction between inflammatory responses and cardiac health is prominent for the development of safer and more efficacious therapies for heart failure patients. The present study, using both acute (lipopolysaccharide) and chronic (high-fat diet) inflammation models, reiterated the adverse effects of abnormal macrophages activation on cardiac function. Our Sectm1a knockout mouse model showed exacerbated cardiac and systemic inflammatory responses, resulting in further aggravation of contractile dysfunction on the heart after endotoxin challenge. We also demonstrated Sectm1a as a new regulator of macrophage function through LXR $\alpha$  pathway. These data suggest a novel approach to regulate macrophage-elicited inflammation.